The effect of inherent and induced anisotropy at boundary value level

Sivasithamparam, N.; Karstunen, M.; Bonnier, P.; Brinkgreve, R.

Publication date
2011

Document Version
Final published version

Published in
Computer Methods for Geomechanics

Citation (APA)
Sivasithamparam, N., Karstunen, M., Bonnier, P., & Brinkgreve, R. (2011). The effect of inherent and induced anisotropy at boundary value level. In *Computer Methods for Geomechanics: Frontiers and New Applications* (pp. 256-261). (Computer Methods for Geomechanics: Frontiers and New Applications; Vol. 1). Centre for Infrastructure Engineering and Safety.

Computer Methods for Geomechanics: Frontiers and New Applications

Volume 1

Editors

Nasser Khalili and Markus Oeser

The University of New South Wales, Sydney, Australia

Typeset by: Olympus Infotech Pvt. Ltd, Chennai, India (www.olympus.co.in)
Published by: Centre for Infrastructure Engineering and Safety
Place of Publication: Sydney, Australia, 2011
ISBN: 978-0-9808244-1-4 (Volume 1)
ISBN: 978-0-9808244-2-1 (Volume 2)
ISBN: 978-0-9808244-3-8 (CD)

IACMAG 2011 – Melbourne, Australia, 9–11 May 2011

The effect of inherent and induced anisotropy at boundary value level

N. Sivasithamparam & M. Karstunen
University of Strathclyde, Glasgow, U.K

P. Bonnier
PLAXIS B.V, Delft, The Netherlands

R. Brinkgreve
Delft University of Technology & PLAXIS B.V, Delft, The Netherlands

Abstract

This paper shows the comparison of two anisotropic models: an advanced rotational hardening model that accounts for both inherent and plastic strain induced anisotropy (S-CLAY1) and the Sekiguchi-Ohta model which accounts for inherent anisotropy only. In the paper, two-dimensional behaviour of a benchmark embankment on soft soils is modelled with the PLAXIS finite element program using user-defined implementations of the S-CLAY1 and Sekiguchi-Ohta models. The same problem is then reanalysed by switching off the evolution in anisotropy in the S-CLAY1 model.

1 INTRODUCTION

Natural soils behave in a highly anisotropic manner due to the deposition process (resulting in inherent anisotropy) and subsequent loading history (induced anisotropy). An accurate description of anisotropy of soft soils is necessary for safe and economic design of structures on soft soil deposits. The models should be relatively simple, easy to understand and ideally, it should be possible to determine the values for the model input parameters from standard laboratory tests. This would namely enhance the confidence of practicing geotechnical engineers for adopting the models for geotechnical analyses.

The S-CLAY1 model (Wheeler et al, 1999; Wheeler et al, 2003; Karstunen and Koskinen 2008) is an extension of the Modified Cam-clay (MCC) model (Roscoe and Burland 1968) with two additional model constants and one additional state variable, required to describe the inherent and plastic strain induced anisotropy. The Sekiguchi-Ohta (SO) model (Sekiguchi and Ohta 1977) is an extension of the original Cam-clay model (Roscoe, Schofield and Wroth 1958) with an inclined yield surface along virgin K_0 consolidation axis. Hence, the model is able to account for inherent anisotropy only. The experimental results by Karstunen and Koskinen (2008) suggest that inclusion of both inherent and induced anisotropy results is very good reproduction in soft soil behaviour at element level, but as yet, it has not been explored what the effect of inherent versus strain induced anisotropy is at a boundary value level.

The first part of this paper gives a short description of the S-CLAY1 and SO models in triaxial stress space. In further sections the geometry of the benchmark embankment is described and results of the finite element simulations are presented, followed by brief conclusions.

2 CONSTITUTIVE MODELING OF ANISOTROPY OF SOFT CLAY

2.1 The S-CLAY1 Model

The S-CLAY1 model was proposed by Wheeler, Karstunen and Näätänen (1999) and is fully described in Wheeler, Näätänen, Karstunen and Lojander (2003). The model is an extension of conventional critical state models, with anisotropy of plastic behaviour represented through an inclined yield surface and a rotational component of hardening, which allows for the development or degradation of fabric anisotropy during plastic straining.

For the simplified conditions of a triaxial test, considering a cross-anisotropic sample, the S-CLAY1 yield function, f_y, can be expressed in terms of the mean effective stress p' and deviator q as:

$$f_y = (q - \alpha p')^2 - (M^2 - \alpha^2)(p'_m - p')p' = 0 \qquad (1)$$

where M is the slope of the critical state line, p'_m defines the size of the yield curve and α defines the orientation of the yield curve, see Figure 1. The scalar parameter α is a measure of the degree of plastic anisotropy of the soil. With $\alpha = 0$ the soil behaviour is inherently isotropic and Equation 1 corresponds to the yield curve in the conventional Modified Cam Clay model.

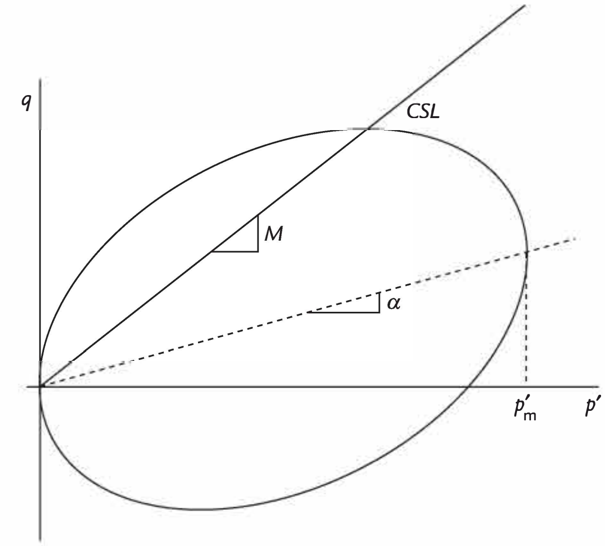

Figure 1 Yield curve of the S-CLAY1 model in triaxial stress space.

The rotational hardening law describes the change of orientation of the yield surface with plastic straining. In triaxial stress space, the hardening law takes the following form:

$$d\alpha = \mu\left(\left[\frac{3\eta}{4} - \alpha\right]\langle d\varepsilon_v^p\rangle + \beta\left[\frac{\eta}{3} - \alpha\right]\left|d\varepsilon_d^p\right|\right) \quad (2)$$

where $d\varepsilon_d^p$ is the increment of plastic deviatoric strain and μ and β are two additional soil constants. The soil constant β controls the relative effectiveness of plastic shear strains and plastic volumetric strains in setting the overall instantaneous target value for α (which will lie between $3\eta/4$ and $\eta/3$), whereas the soil constant μ controls the absolute rate of rotation of the yield surface towards its current target value of α. As for an cross-anisotropic soil the values of α and β, can be theoretically derived based on K_0^{NC} (coefficient of earth pressure in normally consolidated range). As described in Wheeler, Näätänen, Karstunen and Lojander (2003), the model can be easily generalised to 3D, as needed for finite element simulations. Full validation of the model is provided in Karstunen & Koskinen (2008).

2.2 Sekiguchi-Ohta (SO) Model

The original Cam clay model was developed based on isotropically consolidated reconstituted soil samples. Sekiguchi and Ohta (1977) proposed a model for K_0 consolidated clays by changing the yield surface to be centred around the K_0 line. The shape of the SO model accounts, therefore, for the anisotropy developed during K_0 consolidation as shown Figure 2. This model is called the SO inviscid model, as in addition to this model, Sekiguchi and Ohta (1977) formulated a viscid formulation which describes both stress induced anisotropy and time

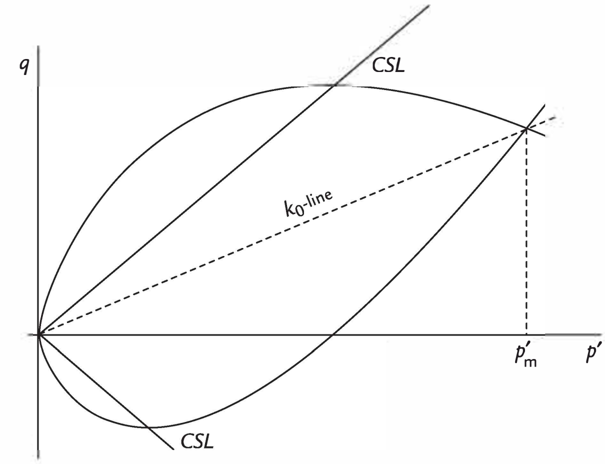

Figure 2 Yield curve of the Sekiguchi-Ohta model in triaxial stress space.

dependency. However, this study considers the inviscid SO model only.

The yield function (f_y) of the SO inviscid model (Sekiguchi and Ohta 1977), can be expressed in triaxial stress space, using the following Equation:

$$f_y = MD\ln\left(\frac{p'}{p'_0}\right) + D\eta_0 - \varepsilon_v^p = 0 \quad (3)$$

where p'_0 is the effective mean stress at the end of K_0 consolidation, η_0 is the stress ratio characterizing stress induced anisotropy, ε_v^p is volumetric plastic strain and D is the coefficient of dilatancy. D is defined as follows:

$$D = \frac{\lambda^* - \kappa^*}{M} \quad (4)$$

where $\lambda^* = \lambda/(1+e_0)$ and $\kappa^* = \kappa/(1+e_0)$ are the modified compression and swelling indexes respectively, and e_0 is the void ratio.

As explained in the Sekiguchi and Ohta (1977) paper, the model can be easily generalised in 3D. If $\eta_0 = 0$, the SO model is reduced to the original Cam-clay model.

3 BENCHMARK EMBANKMENT

The aim of the paper is to explore and understand the differences in predicted soil response caused by inherent and plastic strain induced anisotropy. A benchmark embankment problem is selected to represent a typical geotechnical engineering problem where anisotropy might play a role. Finite element calculations are performed with PLAXIS 2D using S-CLAY1 and SO models which have been implemented as user defined constitutive models.

An embankment constructed on soft soil is assumed to be 2 m high, with a width at the top of 10 m and the side slopes with a gradient of 1:2. The soft soil is assumed to have the properties of soft

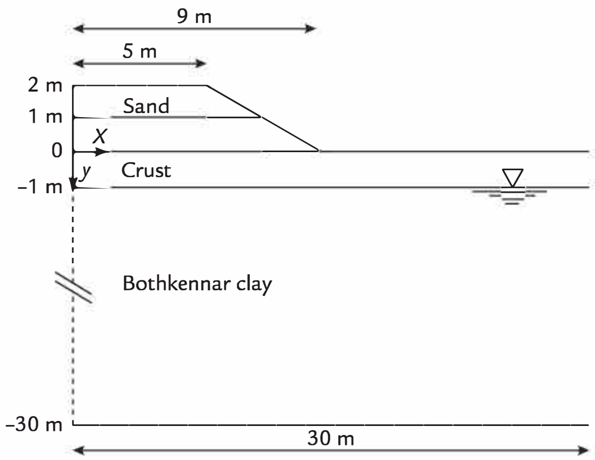

Figure 3 Geometry of benchmark embankment and assumed soil profile.

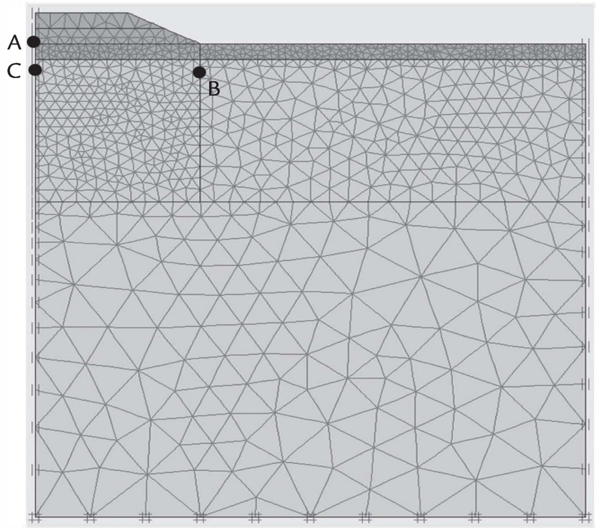

Figure 4 Finite element mesh of the benchmark embankment.

Table 1 Soil parameters of dry crust and sand layer

Parameter	Crust	Sand
γ (kN/m^3)	19.0	20.0
E′ (kPa)	3000.0	40000.0
ν'	0.2	0.35
c′	2.0	0.0
φ'	37.1	40.0
ψ'	0.0	0.0
$k_x = k_y$ (m/day)	8.64E-5	1.0E-3

Bothkennar clay which extends for 29 m depth. At the surface there is a 1 m deep over-consolidated dry crust. The geometry of the embankment is shown is Figure 3. The groundwater table assumed to be located at 1 m below the ground surface. The finite element mesh used in this benchmark embankment is shown in Figure 4.

The embankment, assumed to be made of granular material, was modelled with a simple Mohr-Coulomb model; see Table 1 for material parameters. In order to make the results fully comparable, the

Table 2 The S-CLAY1 model values for state variables, conventional soil constants and additional parameters used to control evolutions of anisotropy for Bothkennar clay

Parameter	Value
Soil constants	
κ	0.02
ν'	0.2
λ	0.3
M	1.51
γ (kN/m^3)	16.5
$k_x = k_y$ (m/day)	2.5E–4
State variables	
e_0	2.0
OCR	1.5
α_0	0.59
Additional anisotropy parameters	
μ	50
β	1

Table 3 The SO model values of state variables and conventional soil constants for Bothkennar clay

Parameter	Value
Soil constants	
κ'	0.00667
ν'	0.2
λ^*	0.1
M	1.51
D	7.1
$k_x = k_y$ (m/day)	2.5E–4
γ (kN/m^3)	16.5
K_0^{nc}	0.397
State variables	
e_0	2.0
OCR	1.5

over-consolidated dry crust layer is also modelled with the Mohr-Coulomb model (see Table 1 for material parameters). This embankment problem is hence expected to be dominated by the soft soil response and is not sensitive to the embankment and dry crust parameters.

Bothkennar clay material has been extensively studied and consistent set of laboratory data is available to derive material parameters for the S-CLAY1 and the SO model (e.g., Géotechnique Symposium-in-Print 1992, McGinty 2006, McGinty et al. 2008) in a consistent manner. Table 2 gives the values for the initial state variables as well as the conventional soil constants for Bothkennar clay as required for the S-CLAY1 model. Table 3 gives the material parameters for Bothkennar clay used to simulate the SO model. Based on the λ and κ values, and the initial void ratio, λ^* and κ^* can be calculated for the SO model (correspondingly $\lambda^* = 0.10$ and $\kappa^* = 0.0067$). The permeability k is assumed to be the same in the vertical and horizontal direction for the sake of simplicity.

The S-CLAY1S model (Karstunen et al. 2005), which account additionally for the effect of bonding and destructuration, was first implemented to the PLAXIS finite element program as user-defined soil model by Wiltafsky (2003). The model can be reduced to the S-CLAY1 model through suitable parameter selection.

The current version of the S-CLAY1S model which used in this study is implemented as a user-defined soil model in to PLAXIS by the first Author using an improved numerical algorithm. The SO model was also implemented to PLAXIS program as a user-defined soil model by the first Author.

The analysis was performed using small deformation assumption as the idea is just to compare the two models at boundary value level. The construction of the embankment was simulated by two undrained phases of 5 days each. In all analyses, drained conditions and zero initial pore pressures have been assumed above the water table. For the initial condition, the in-situ K_0 value was assumed to be $K_0 = 0.5$ due to overconsolidation of Bothkennar clay. The first construction phase, in which the first layer of the embankment was built, was followed by a 30 day consolidation stage. After the completion of the second layer of embankment, the final consolidation was simulated until the maximum excess pore pressure has reduced to 1 kPa (i.e. practically full dissipation of excess pore pressures).

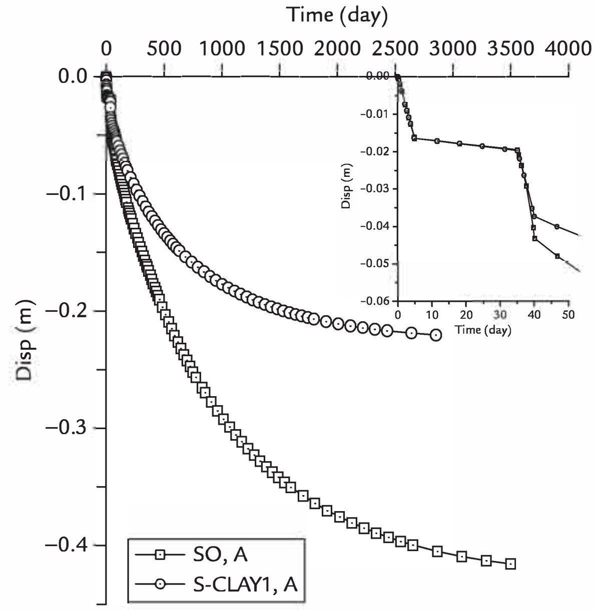

Figure 5 Comparison of time settlement curves at point C.

4 RESULTS OF NUMERICAL ANALYSIS

The comparison between the results of the finite element simulations are presented in Figures 5–9, using different symbol types for the different models (S-CLAY1 and SO). The settlement predictions

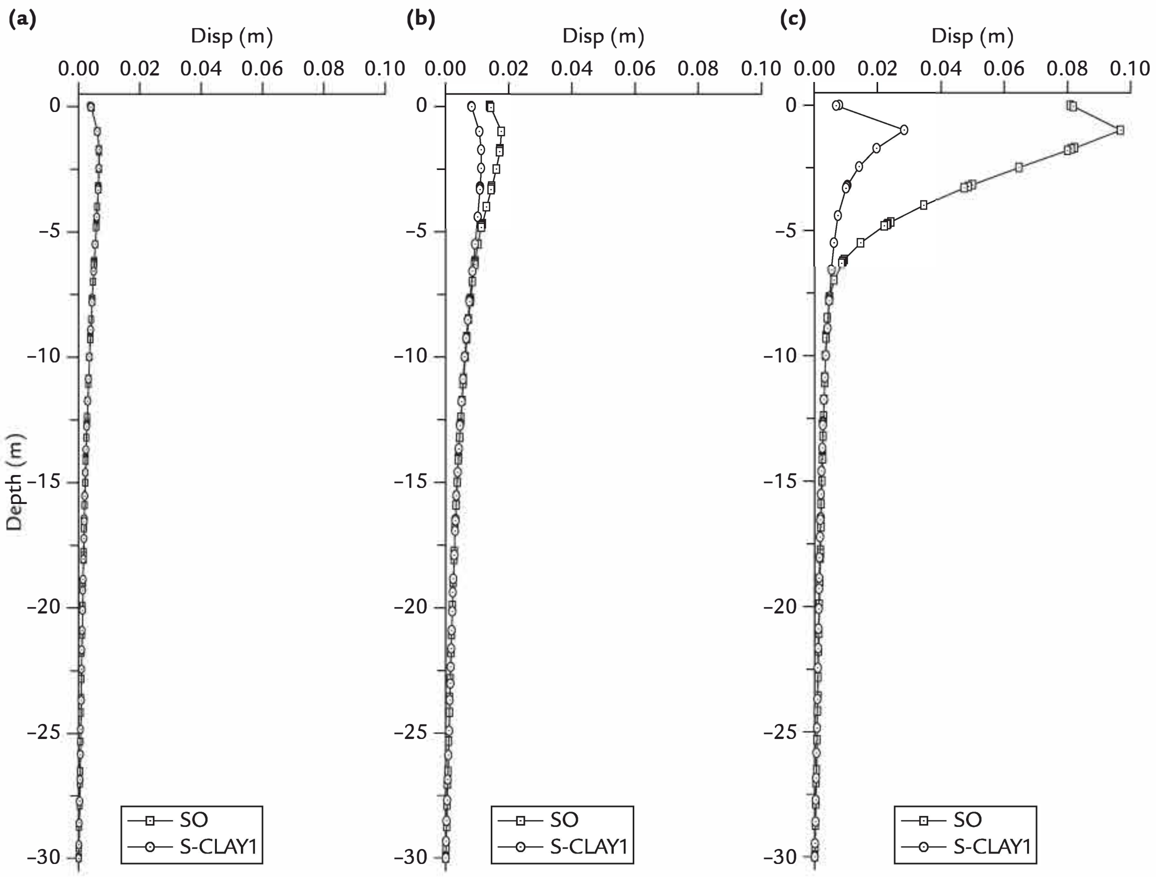

Figure 6 Final horizontal displacement predictions at the embankment toe: (a) immediately after 1st layer construction; (b): immediately after 2nd layer construction; (c): end of consolidation.

versus time at the node directly under the centreline of the embankment (point A in Figure 4) are presented in Figure 5 until the end of consolidation (maximum excess pore pressure 1 kPa). The SO model gives highest prediction of about 0.4 m (corresponding to 9.5 years), whilst S-CLAY1 model gives estimate of about 0.2 m (corresponding to 8 years) for the final vertical settlement. The predictions by the SO are almost double of the final vertical settlements predicted by the S-CLAY1 model. This significant difference in the predicted vertical settlement starts after the construction of the 2nd layer of embankment; see small zoomed curves in Figure 5.

In Figure 6, the predicted horizontal displacements versus depth under the toe of the embankment are presented. Until the construction of 2nd layer, both models give almost identical predictions of the horizontal displacements (Fig. 6(a), and (b)), but at the end of consolidation, the SO model predicts significantly larger horizontal displacement (almost 3.5 times higher) than the S-CLAY1 model (Fig. 6 (c)).

The excess pore pressure versus time profile predicted underneath the centreline of the embankment (point C in Figure 4, 2 m below the ground surface) and underneath the toe of the embankment (point B in Figure 4, 2 m below the ground surface) until end of consolidation is shown in Figure 7. The SO model predicts considerable excess pore pressure just after the construction of 2nd layer of embankment. Because both models implicitly based on model input predict the same K_0 value, underneath the centerline both models predict very similar stress paths. Differences between the models hence come from modeling areas around the toe of the embankment where S-CLAY1S predict significant evolution on anisotropy.

In the S-CLAY1 model, it is possible to switch off the plastic strain induced anisotropy, by giving the soil constant μ a value of zero. In Figures 8–9, the impact between inherent and induced anisotropy is studied. The comparisons of settlement curves with time underneath the centreline (point A) are shown in Figure 8. Ignoring changes in anisotropy results in higher predicted settlements than in the case when it is included, however, the settlements still are significantly smaller than predicted by the SO model. In Figure 9, the comparison of surface settlement predictions at the end of the consolidation is presented for S-CLAY1 and S-CLAY1 with α = constant. In all the comparisons, the model that ignores strain-induced anisotropy (S-CLAY1 with α = constant) results in higher predicted deformations than predicted by the S-CLAY1 model. This demonstrates that the plastic work is associated with the evolution of fabric in the S-CLAY1 model reduces the overall deformations.

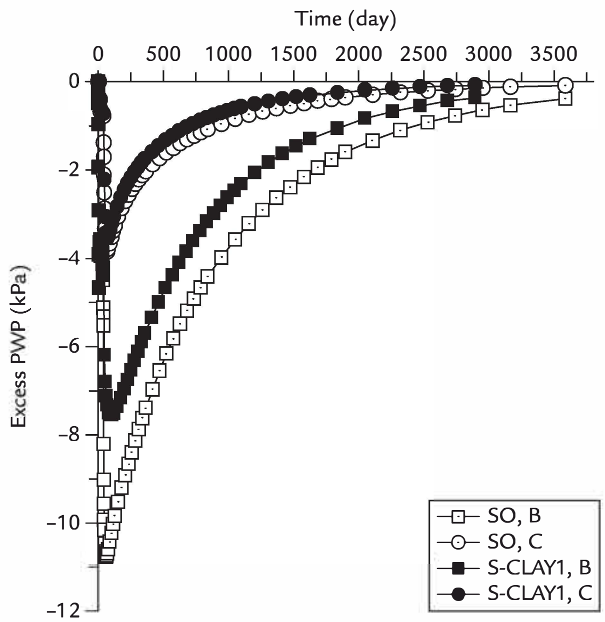

Figure 7 Excess PWP at the point B and C with time.

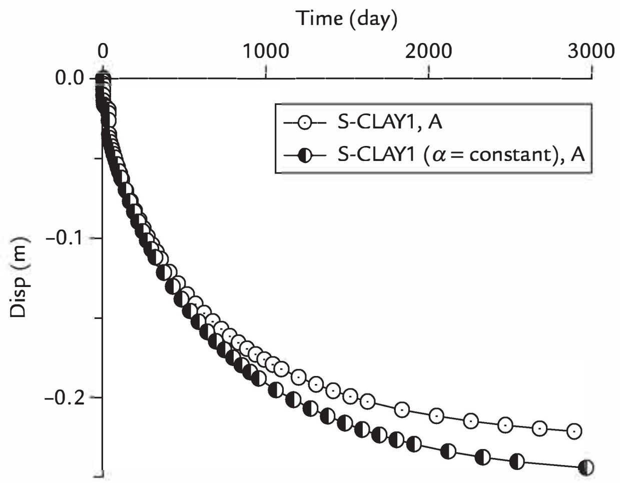

Figure 8 Comparison of time settlement curves at point C.

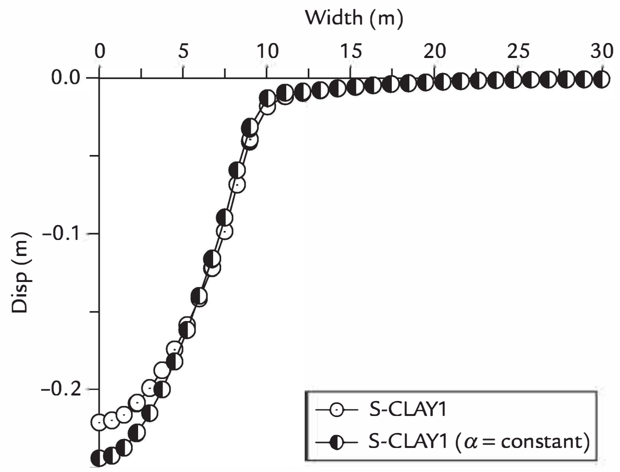

Figure 9 Surface settlement curves at the end of analyses.

5 CONCLUSIONS

The paper studies the influence of the inherent and induced anisotropy by comparing model simulation using the S-CLAY1 model (Wheeler et al, 1999; Wheeler et al, 2003; Karstunen and Koskinen 2008) that accounts for both inherent and plastic strain induced anisotropy, and the classical Sekiguchi-Ohta model (Sekiguchi and Ohta 1977) which incorporates only inherent anisotropy by simulating a benchmark embankment on soft Bothkennar clay. The model simulations demonstrate that the inclusion of evolution of anisotropy results in a notable reduction in the predicted vertical and lateral deformations in comparison with the models that ignore the effect of plastic strain induced anisotropy. Furthermore, even when the evolution of anisotropy is ignored, the results are heavily influenced by the particular form assumed for the yield surface. Overall, the SO model predicts significantly larger vertical and horizontal deformations than the S-CLAY1 model. Further work will involve comparing the performance of the models against experimental data and instrumented test structures.

6 ACKNOWLEDGEMENTS

The work presented was sponsored by the Academy of Finland (Grant 1284594) and the European Community through the programme "People" as part of the Industry-Academia Pathways and Partnerships project GEO-INSTALL (PIAP-GA-2009-230638).

REFERENCES

Géotechnique Symposium-in-Print (1992). Géotechnique 42 (2).

Karstunen, M. and Koskinen, M. (2008). Plastic anisotropy of soft reconstituted clays. *Can. Geotech. J.* 45, No. 3, 314–328.

Karstunen, M., Krenn, H., Wheeler, S.J., Koskinen, M., Zentar, R. (2005). Effect of anisotropy and destructuration on the behaviour of Murro test embankment. *ASCE Int. J. Geomech.*, 5(2), 87–97.

McGinty, K. (2006). *The stress-strain behaviour of Bothkennar clay*. PhD thesis, Department of Civil Engineering, University of Glasgow, UK.

Roscoe, K. H. and Burland, J. B. (1968).*On the generalized stress- strain behaviour of wet clay*, Engineering plasticity, Cambridge Univ. Press, Cambridge, UK, pp. 553–609.

Roscoe, K. H., Schofield, A. N., Wroth, C. P. (1958), On the Yielding of Soils, *Geotechnique* 8: 22–53.

Sekiguchi, H. & Ohta, H. (1977). Induced anisotropy and time dependency in clays. *Proc. 9th Int. Conf. Soil Mech. Found. Engng*, Tokyo, 229–238.

Wheeler, S., Karstunen, M. & Näätänen, A. (1999). Anisotropic hardening model for normally consolidated soft clay. Proc. 7th Int. Symp. on Numerical Models in Geomechanics (NUMOG VII), 33–40.

Wheeler, S. J., Näätänen, A., Karstunen, M. & Lojander, M. (2003). An anisotropic elasto-plastic model for soft clays. *Can. Geotech. J.* 40, No. 2, 403–418.

Wiltafsky, C. (2003). S-CLAY1S, User Defined Soil Model, Documentation, University of Glasgow, UK.